ANALYTICA CHIMICA ACTA 606 (2008) 98–107

available at www.sciencedirect.com

ScienceDirect

journal homepage: www.elsevier.com/locate/aca

Multiplexed high-throughput electrokinetically-controlled immunoassay for the detection of specific bacterial antibodies in human serum

Yali Gao[a], *Philip M. Sherman*[b], *Yu Sun*[a], *Dongqing Li*[c,*]

[a] *Department of Mechanical and Industrial Engineering, University of Toronto, 5 King's College Road, Toronto, Ontario M5S 3G8, Canada*
[b] *Hospital for Sick Children, Departments of Paediatrics and Laboratory Medicine & Pathobiology, University of Toronto, Toronto, Ontario, Canada*
[c] *Department of Mechanical Engineering, Vanderbilt University, Nashville, TN, USA*

ARTICLE INFO

Article history:
Received 11 August 2007
Received in revised form
19 October 2007
Accepted 23 October 2007
Published on line 6 November 2007

Keywords:
Electrokinetic
Microfluidics
Immunoassay
Lab-on-chip
Escherichia coli O157:H7
Helicobacter pylori

ABSTRACT

In previous studies we have developed a simple electrokinetically-controlled lab-on-a-chip for heterogeneous immunoassay. In that method, all the sequential operations in an immunoassay, such as reagent loading and washing, were performed automatically by electrokinetically controlling the flow in an H-shaped microchannel. Here, we demonstrated further development of a high-throughput immunoassay microfluidic chip, and the application of the new immunoassay microfluidic chip in assaying human serum. The microfluidic immunoassay analyzed ten samples in parallel in 22 min. Bacterial antibodies in samples were captured by antigens pre-patterned on the bottom wall of a microchannel and then bound with TRITC-labeled detection antibodies to generate fluorescent signals. With optimized surface concentration of antigen, the assay detected *Escherichia coli* O157:H7 antibody and *Helicobacter pylori* antibody from buffer solutions in concentration ranges of 0.02–10 $\mu g\,mL^{-1}$ and 0.1–50 $\mu g\,mL^{-1}$, respectively. Human sera that were *E. coli*-positive or *H. pylori*-positive were accurately distinguished from respective negative controls. Moreover, the two antibodies, anti-*E. coli* and anti- *H. pylori* antibodies, could be simultaneously detected from human serum. This electrokinetically-controlled immunoassay shows an excellent potential for efficiently detecting multiple pathogenic infections in clinical environments.

1. Introduction

With the rapid development of micro-total analysis system (μ-TAS) since the 1990s, microfluidics has proven to be a powerful platform for a variety of biological assays [1], such as DNA analysis [2], immunoassay [3], protein assays [4,5] as well as cell analysis [6]. In particular, immunoassay, one of the most important biochemistry analyses based on highly specific antibody-antigen interactions, has been an appealing application area of microfluidics techniques over the last decade. Extensive research in this field has clearly demonstrated the advantages of miniaturization, such as improved reaction kinetics, reduced consumption of costly samples and reagents, flexible design and portable system [3]. Continuous

* *Corresponding author*. Tel.: +1 615 322 8601; fax: +1 615 343 6687.
E-mail address: dongqing.li@vanderbilt.edu (D. Li).
0003-2670/$ – see front matter © 2007 Elsevier B.V. All rights reserved.
doi:10.1016/j.aca.2007.10.052

advances in the μ-TAS field and growing requirements for bioassays have shifted the paradigm in recent years towards the development of high-throughput(multi-sample) [7], multiplexed (multi-analyte) [8–10], parsimonious [7,10–12], automated [13,14] and ultrasensitive [15–17] immunoassays. Particularly, high-throughput is generally desirable, as samples for immunoassay, whether in biochemical studies or clinical environments, are usually in large quantities.

The realization of high-throughput microfluidic immunoassay has been explored using different systems. For instance, Sato et al. constructed a sandwich immunoassay microfluidic chip with branching channels to process four samples simultaneously with only one pump [18]. Lai et al. designed a compact disk-like microfluidic device for enzyme-linked immunosorbent assay (ELISA) with which multiple assays on one disk can be operated in parallel by controlling flow sequence through centrifuge pumping and capillary valving [19]. Rowe et al. developed an array immunosensor, the operation of which includes the patterning of capture antibodies onto a waveguide using six vertical channels, and subsequent pumping of samples and detection antibodies through six horizontal channels. Localized immunoreactions at the intersections generate a 6×6 matrix of signals [8]. Delamarche and co-workers [20,21] developed a "micromosaic immunoassay" using a similar two-step approach, in which the flow of sample and reagent solutions in 20-μm wide silicon microchannels is driven by capillary forces. A two-step approach has also been employed by Jiang et al. in designing a serially diluted immunoassay [22]. The attractiveness of this two-step approach is that, with different probe molecules, multiple analytes can be screened simultaneously from each sample, while multiple samples are being tested at a time. In this way, the cost of time, reagent and labor can be dramatically economized. Kartalov et al. recently developed a high-throughput, multi-antigen microfluidic immunoassay system with built-in valves for fluidic control, so that the entire assay, from capture antibody immobilization to immunoreactions, can be conducted using one microfluidic chip [10]. In spite of these achievements, no study has yet reported on high-throughput heterogeneous immunoassays based on an electrokinetically-driven flow system.

Compared with other flow systems, a critical advantage of electrokinetically-driven flow is the fluidic control without external valves. That is, pumping and fluidic control are realized at the same time, and flow switching is as easy as changing an applied electric field. This advantage is especially desirable for conducting a multi-step analysis like immunoassay, where the sequential steps can be readily integrated and the whole process automated. In addition, the micro-devices are compact, without the need for external pumps, tubing and valves. These advantages have been manifested in the various integrated electrokinetically-controlled microfluidic devices [23], such as microfluidic chips for enzyme assay [24,25] and homogeneous immunoassay [26,27].

In our laboratory, studies have pursued the development of heterogeneous immunoassay based on electrokinetically-driven flow [28–31]. We have successfully developed an multiplexed electrokinetically-controlled microfluidic immunoassay using a two-step (coating + assay) design [28]. Based on that work, we have now built the function of high-throughput analysis into the immunoassay chip. Compared with most other high-throughput microfluidic immunoassay, the advantage with this immunoassay microchip is not only that the assay is automatically conducted, but also, the microfluidic network is highly integrated, which brings about reduced consumption of reagents, minimized manual work, as well as small footprint of the device.

A targeted application of our microfluidic immunoassay is in clinical setting. Therefore, verification of its feasibility to evaluate clinical samples is crucial. This is because clinical fluids can behave differently from pure synthetic samples due to a variety of reasons, such as matrix effects and cross-reaction of the complex constituents with probe molecules [32]. In the only previous paper on electrokinetically-driven heterogeneous immunoassay for testing clinical samples, Linder et al. reported strong matrix effects when human serum was tested for immunoglobulin (Ig)G. The authors suggested that the interactions of serum components with channel walls could interfere with electrokinetic delivery of analytes to the reaction site [33]. It is, therefore, important to conduct further investigations to determine whether an electrokinetically-driven flow system is an appropriate platform for heterogeneous immunoassays to be employed for clinical diagnostic purposes.

This paper describes our study on the development of an electrokinetically-controlled, high-throughput immunoassay for testing multiple clinical samples against multiple pathogen targets. We have adopted a non-competitive, indirect configuration. That is, antibody molecules in the samples were captured by immobilized antigen and then bound by TRITC-conjugated detection antibody. Two clinically important microbial pathogens, *Escherichia coli* O157:H7 and *Helicobacter pylori*, were studied as model analytes. *E. coli* O157:H7 is recognized as a major cause of hemorrhagic colitis and can induce other life-threatening diseases [34]. *H. pylori* infects half of the world's population and causes gastritis, peptic ulcer disease [35] and gastric cancers [36]. The microfluidic immunoassay was first tested with synthetic samples and then applied to assay human sera for the infection status of either pathogen. Simultaneous screening for both analytes was also conducted.

2. Experimental

2.1. Materials

The procedures for preparing bacterial antigens of *E. coli* O157:H7 and *H. pylori* were described previously [37,38]. Lysate antigens were diluted to final concentrations of 6–1000 $\mu g\,mL^{-1}$ using a pH 9.6 carbonate buffer (consisting of 0.03 M $NaHCO_3$ and 0.02 M Na_2CO_3). The assay buffer was Tris–HCl (25 mM, pH 7.5). Bovine serum albumin (BSA) from Sigma–Aldrich (Oakville, Ontario, Canada) was diluted to concentrations of 5% and 10% (w/v) in Tris–HCl buffer to be used as blocking and diluent buffer. A 10% BSA solution was used in the assays of human serum, whereas a 5% BSA solution was used in all other assays. Polyclonal rabbit anti-*H. pylori* antibody and polyclonal goat anti-*E. coli* O157:H7 antibody were obtained from DAKO (Glostrup, Den-

mark) and KPL (Gaithersburg, MD), respectively. Detection antibodies, including TRITC-conjugated donkey anti-rabbit IgG, TRITC-conjugated donkey anti-goat IgG and TRITC-conjugated donkey anti-human IgG, were all purchased from Jackson ImmunoResearch Laboratories, Inc. (West Grove, PA). Anti-rabbit IgG and anti-human IgG were used at a dilution of 1:25 (IgG concentration of 60 $\mu g\,mL^{-1}$) and anti-goat IgG was used at a dilution of 1:100 (IgG concentration of 15 $\mu g\,mL^{-1}$). Human sera post *H. pylori* or *E. coli* O157:H7 infection as well as control samples were collected in two earlier studies [39,40]. The *H. pylori* or *E. coli* status of the samples was determined by validated ELISA [39] and immunoblot assay [40], respectively. Ultrapure water from Millipore water purification system (Molsheim, France) was used to prepare all solutions.

2.2. Chip preparation

Two different microfluidic networks (μFNs) were used in the immunoassay experiments. The one used for antigen immobilization consisted of five separate channels (100 μm wide, 60 μm high) with a parallel region, as shown in Fig. 1a. The other μFN used directly for the immunoassay was composed of ten channels each connected with a sample well, one channel connected with detection antibody well, one with buffer well and one with waste solution well, as shown in Fig. 1b. The linear region of the array of ten sample channels was designed as the reaction region. The width of the sample channels was 50 μm each, while other channels in this network were all 500 μm wide. In this way, the ten sample channels connected in parallel had an equal flow resistance per unit length with the other channels, thereby ensuring a moderate flow rate over the entire μFN. To minimize undesirable pressure-driven flow, the height of the μFN was only 8 μm. The overall dimension of the μFN was 16 mm × 24 mm.

Microfabrication was done by using soft lithography, as described previously [28]. Antigen immobilization procedures were also similar to those used previously [28]. Briefly, the PDMS replica for antigen patterning was plasma-retreated and brought into conformal contact with a PDMS-coated glass microscope slide, as shown in Fig. 1a. Immediately thereafter, 0.5 μL of antigen solution was added to one end of each channel and the channels were wetted spontaneously. The chip was then covered with a piece of micro cover glass and incubated at room temperature (22–25 °C) for 15 min. After incubation, the chip was placed under a deep vacuum (−20 in.Hg) to evaporate the solvent. Then, the PDMS slab was peeled off, and the chip was rinsed with water and dried under a gentle blow of nitrogen. A monolayer of antigen was patterned onto the surface at this stage. The PDMS replica for immunoassay was plasma-treated and put into conformal contact with this antigen-patterned substrate, with the parallel part of the sample channels crossing the lines of antigen pattern perpendicularly, as shown in Fig. 1b. The matrix of rectangular intersections became reaction regions when the assay was conducted, as illustrated in the enlargement. After the chip was formed, blocking solution was loaded in and incubated for 15 min at room temperature.

2.3. Electrokinetically-driven immunoassay

In the immunoassay experiments with synthetic samples, sample solutions were either *E. coli* O157:H7 antibody or *H. pylori* antibody diluted using diluent buffer containing 5% BSA. Detection antibodies were also diluted using 5% BSA solution. In assaying human sera, sample solutions were mostly human sera diluted to 1:100 using 10% BSA solution, with an exception in the simultaneous detection of both anti-*E. coli* and anti-*H. pylori* antibodies (result shown in Fig. 7). The ten samples of

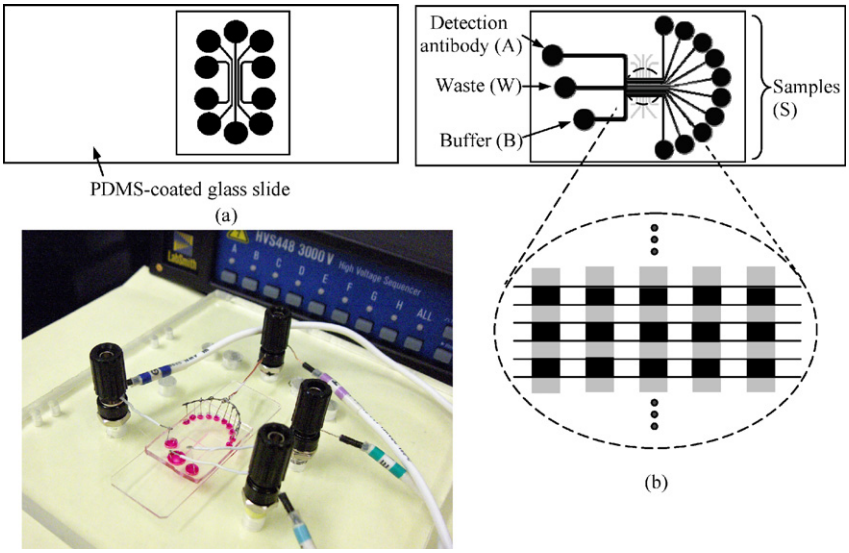

Fig. 1 – Preparation process of the electrokinetically-controlled immunoassay. (a) Antigen was immobilized onto a PDMS-coated glass microscope slide by using a μFN; (b) The μFN (schematic not proportional to actual size) for immunoasay was placed over the patterned antigen (in gray). The matrix of rectangular intersections became reaction regions in the assay. (c) A picture of the microfluidic chip being connected by electrodes with the output cables of a high-voltage sequencer. The wells of the chip were filled with dye to illustrate the geometry.

human sera used in that experiment were (diluted using 10% BSA): S1 – *H. pylori*-positive serum, diluted to 1:100 (*H. pylori*_P1, 1:100), S2 – *H. pylori*_P2, 1:100, S3 – *H. pylori*_N1, 1:100 (*H. pylori*-negative serum), S4 – *E. coli*_P1, 1:100, S5 – *E. coli*_P2, 1:100, S6 – *E. coli*_N1, 1:100, S7 – *E. coli*_N2, 1:100, S8 – *H. pylori*_P1 + *E. coli*_P1, 1:100, S9 – *H. pylori*_P2 + *E. coli*_P2, 1:100. S10 – diluent buffer, a negative control. The net dilution of serum was 1:50 for S8 and S9.

After the blocking step, 8 μL of each sample, 30 μL of detection antibody, 30 μL of diluent buffer, and 50 μL of Tris–HCl buffer were added to the wells for sample, antibody, buffer and waste, respectively, which had been punched at different sizes ($\phi_S = 2.5$ mm, $\phi_A = \phi_{\equiv} = 4.8$ mm, $\phi_W = 6.3$ mm). Using a big waste well helped reduce hydrostatic pressure difference during the assay, so as to minimize pressure-driven flow. Platinum electrodes were then placed into the wells and the assay ready to run. A picture of the chip at this stage is presented in Fig. 1c.

The electrokinetically-driven immunoassay was conducted at room temperature. The process was composed of seven steps – loading, incubation, and two steps of washing of sample solutions, followed by loading, incubation and washing of detection antibody. Incubation time for sample and antibody was 10 min and 5 min, respectively.

The flow paths of solutions in each step were designed as shown in Fig. 2. Flow route in the two successive steps of loading and incubation was the same, for the operation of both sample and antibody solutions. In addition to the major flow to deliver the reactant, sometimes a minor auxiliary flow was added. For example, in Fig. 2b and d, a minor flow towards the waste well countered possible pressure-driven flow from the waste well to the reaction region. Also, in Fig. 2c, minor flows from the sample wells and buffer well served to confine the fluid toward the waste well only.

Based on the flow routes, the applied electric potentials in each step were determined first by taking the μFN as a network of electric resistors and estimating the potentials according to the Kirchhoff's rules [24,41]. Then, numerical simulation of the microfluidic transport processes (details described below) was conducted to optimize the potential values, following a trial-and-error approach. Once the applied electric field for a loading or washing step was determined, the duration of the step was decided from the simulation of the transient mass transportation. Theoretically, a loading/washing process was complete when the reactant was delivered into/out of the reaction region. In practice, the durations of the steps were extended to ensure thorough solution dispensing.

The immunoassay experiments were conducted automatically by using a high-voltage sequencer (Labsmith, Livermore, CA). The controlling parameters, i.e., the applied electric potentials and duration for each step, were pre-set with Sequence software (Labsmith, Livermore, CA). After the sequencer was triggered on, all operations were automatically conducted and switched.

2.4. *Numerical simulation*

Physical modeling of the electrokinetic transport processes includes the Laplace's equation for electric field, 2-D Navier–Stokes equations for flow field, and transient mass transport equation for reactant concentration field, as described in our past study [30]. However, due to the similitude between the velocity field and electric gradient field for the EOF considered here [42], the velocity field can be directly obtained from the electric field using the relationship $\vec{V}_{eo} = \mu_{eo}\vec{E} = -\mu_{eo}\nabla\Phi$, thus eliminating the necessity of solving the non-linear Navier–Stokes equations. The simplified 2-D model was described below.

The applied electrical potential, Φ, is described by the Laplace's equation,

$$\nabla^2\Phi = 0 \tag{1}$$

The concentration field of reactant is described by the transient mass transportation equation,

$$\frac{\partial C_i}{\partial t} + (\vec{V}_{eo} + \vec{V}_{ep}) \cdot \nabla C_i = D_i\nabla^2 C_i \tag{2}$$

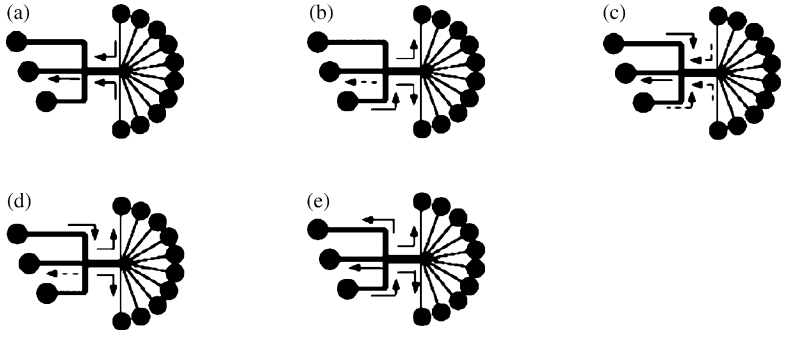

Fig. 2 – Steps in the electrokinetically-controlled immunoassay (schematics are proportional to actual size). The undistinguished parallel region of the ten sample channels is a result of low-resolution printing. Arrows indicate flow direction. Solid arrows stand for major flows, and dashed arrows, minor flows. (a) Loading and incubation of samples. Sample solutions were dispensed from the sample wells to the reaction region and discharged into the waste well. (b) Washing of samples. Buffer solution flushed sample solutions from the reaction region back into the sample wells. (c) Second washing of samples. Sample solutions having entered the antibody channel during the previous three steps were flushed into the waste well. (d) Loading and incubation of detection antibody. (e) Washing of detection antibody.

where C_i is the concentration of the ith sample (e.g. anti-bacterial antibody or detection antibody), $\vec{V}_{eo} = \mu_{eo}\vec{E} = -\mu_{eo}\nabla\Phi$, $\vec{V}_{ep}$ the electrophoretic velocity of the protein molecules calculated by $\vec{V}_{ep} = \mu_{ep}\vec{E} = -\mu_{ep}\nabla\Phi$, D_i the diffusion coefficient of the ith sample.

Boundary conditions for Eqs. (1) and (2) are,

$$\text{at inlets,} \quad \Phi = \Phi_i, \quad C_i = C_{i0};$$

$$\text{at outlets,} \quad \Phi = F_i, \quad \vec{n}\cdot(D\nabla C_i) = 0;$$

$$\text{at walls,} \quad \vec{n}\cdot\nabla\Phi = 0, \quad \vec{n}\cdot[D\nabla C_i - C_i(\vec{V}_{eo} + \vec{V}_{ep})] = 0.$$

where Φ_i is the electrical potential applied at each well, $\vec{n}$ the unit normal vector to the surface. In computing the reactant concentration, the distribution of concentration obtained from a previous step was used as the initial condition of the next step.

The above differential equations were solved by using a commercial software package, COMSOL Multiphysics 3.2, which is based on Finite Element Method.

2.5. *Signal acquisition*

Fluorescent signals were detected by using a Leica DM-LB fluorescence microscope. Images were captured by using a Retiga 12-bit cooled CCD camera (QImaging, Surrey, BC, Canada) at an exposure time of 2 s.

Uneven illumination was compensated for by applying shading correction to captured images. This was performed by standardizing pixel intensities against those from a reference image of a homogeneous fluorescent area, according to

$$D(x, y) = S(x, y) \times \frac{\bar{R}}{R(x, y)}$$

where D is the destination image and S the source image, R the reference image and $\bar{R}$ the mean grayscale of the reference image.

Fluorescent intensities were analyzed by using ImageJ software (NIH, Bethesda, MD). Mean intensities from both the rectangular reaction regions and neighboring background regions were obtained. Signal intensity of each reaction site was then determined as the difference between its own intensity and the average intensity of the two neighboring dark regions.

3. Results and discussion

3.1. *Assay design and numerical simulation*

Unlike that in many other high-throughput microfluidic immunoassay where the parallel assay units are independent from one another [8,11,19], the μFN in the electrokinetically-controlled immunoassay is a highly integrated one, with one well for detection antibody, one well for buffer and one well for waste solution shared among all the samples. With this compact microdevice, the consumption of reagent solution is significantly reduced and manual solution operations in preparing the assay are minimized. Designing the integrated parallel assay chip, consequently, involved special considerations.

An important consideration is that cross-contamination among the samples must be prevented during the assay, i.e., the reaction within each channel should be from the corresponding sample solution only. This consideration was implemented in the following design elements. First, the reaction region was upstream of the intersection of the sample channels during sample loading and incubation, so that each sample solution was dispensed over the reaction site inde-

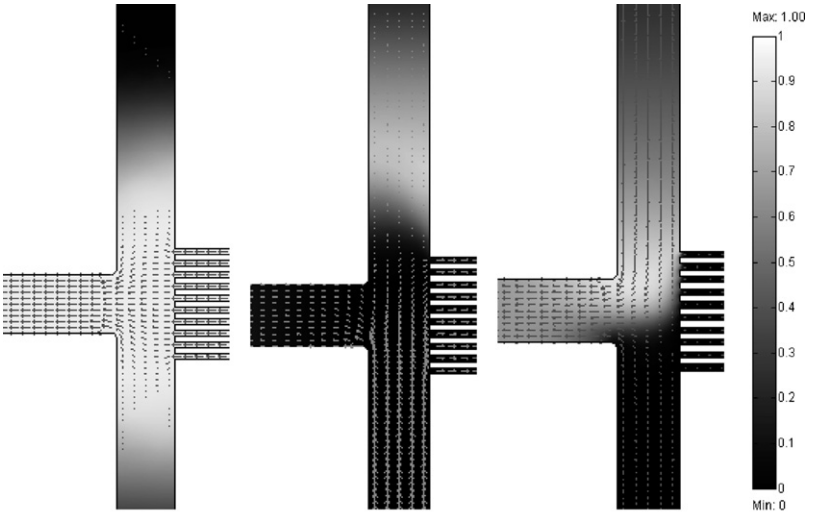

Fig. 3 – The numerical simulation results of sample concentration field at the intersection region. Arrows in the figures denote the flow field. t is the time after the step begins. The concentration bar on the right, with the max and min concentration being 1 and 0, is for figures (a) and (b). For (c), the maximum concentration is 0.3 for higher visual clarity. The reduced concentration was resulted from dispersion of samples.

Table 1 – Controlling parameters in the electrokinetically-controlled immunoassay

Step	Applied electric voltage (V)				Duration (min)
	ϕ_S	ϕ_A	ϕ_B	ϕ_W	
1. Sample loading	330	117	117	0	1
2. Sample incubation	165	59	59	0	10
3. Sample washing	0	150	360	120	1.5
4. Second washing	300	500	300	0	0.5
5. Antibody loading	0	435	182	200	2
6. Antibody incubation	0	217	91	100	5
7. Antibody washing	0	0	600	120	2

pendently before mixing with others. Second, the ten sample channels and the buffer channel were intersected at the same point, so that sample solutions mixed at the intersection would not be flushed back to the reaction regions during the sample washing step. Third, the addition of a second sample-washing step. As illustrated by the results from numerical simulation in Fig. 3, during the first sample-washing step, some mixed sample solution accumulated at the intersection was pushed into the antibody channel. This mixed solution had to be flushed into the waste well, as shown in Fig. 3c, lest it entered the sample channels during antibody loading.

Targeted at the flow patterns shown in Fig. 2, controlling parameters for every step of the assay were determined by using numerical simulation and are summarized in Table 1. In the computation, the value of μ_{eo} and μ_{ep} were $1.6 \times 10^{-8}\,m^2\,V^{-1}\,s^{-1}$ and 0, respectively, as measured in an earlier study [28]. The diffusion coefficient of antibody was $4.0 \times 10^{-7}\,cm^2\,s^{-1}$. To reduce Joule heating, the electric field strength in all loading and washing steps was mostly kept below $150\,V\,cm^{-1}$. The corresponding flow velocity was $240\,\mu m\,s^{-1}$, which is calculated as the product of electrokinetic mobility and electric field strength, i.e., $\vec{V}_{ek} = \mu_{ek}\vec{E} = (\mu_{eo} + \mu_{ep})\vec{E}$. During incubation, flow pattern was kept unchanged from the preceding loading step, but electric field was reduced by half to lower Joule heating.

The durations of incubation for sample and antibody were set as 10 min and 5 min, respectively. For the microfluidic immunoassay in this study, incubation time of 5–10 min should be adequate for the immunoreaction to reach or approach the equilibrium stage, from reported theoretical [43,44] and experimental [15,21,45] studies conducted at comparable conditions. From our preliminary experiments (data

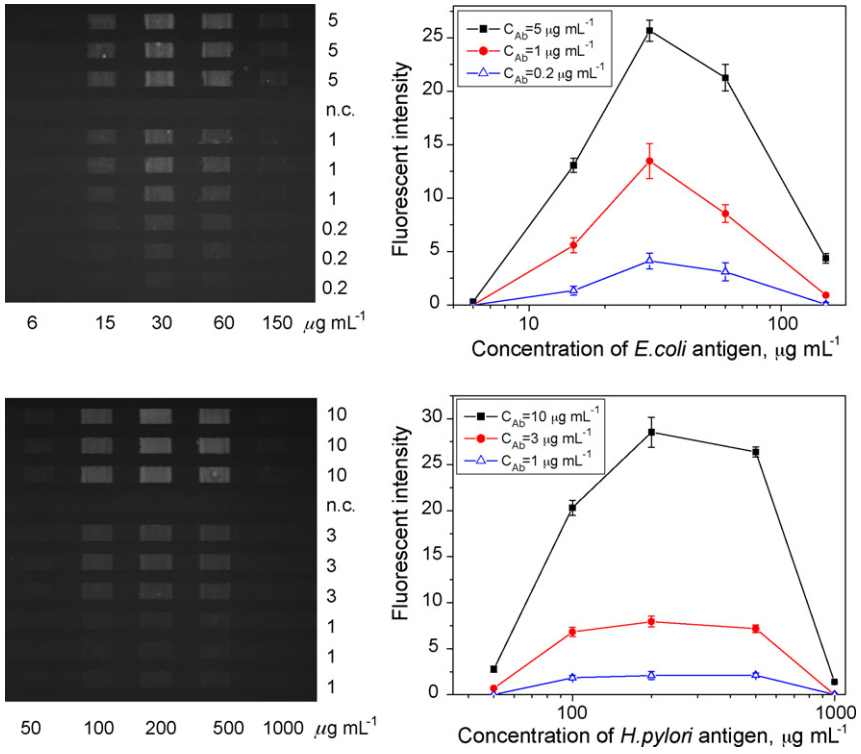

Fig. 4 – Signal intensity as a function of antigen concentration. (a) Fluorescent image for *E. coli* O157:H7 test. Concentrations of coating lysate antigen are indicated at the bottom of the image, and concentrations of *E. coli* antibody on the right hand side of the image. The negative control (4th channel from top) was diluent buffer containing no antibody. (b) Quantified results of each three duplicates. Error bars represent standard error of the mean (S.E.M.). (c, d) Fluorescent image and quantified results for the *H. pylori* test.

not shown), a 10-min sample incubation enhanced the binding reaction and lowered the limit of detection, compared to a 5-min incubation, and therefore was adopted. Detection antibody was at a high concentration (15–60 μg mL^{-1}) and thus the reaction should proceed fast. Incubate time was then set as 5 min, which has been used before and shown to provide sufficient sensitivity [28,29]. The duration of the entire assay was 22 min.

3.2. *Optimization of antigen coating condition*

Optimal performance of an immunoassay depends primarily on an appropriate surface density of probe molecules. Therefore, we first optimized the antigen coating condition, by seeking the optimal concentration of antigen under a fixed coating time of 15 min. Immunoassay experiments were conducted with varied antigen concentrations applied in the five coating channels. Three different concentrations of antibodies, each in a duplicate of three, plus one negative control (diluent buffer), were used as the ten test samples.

Test results are presented in Fig. 4, in which (a) and (b) are the fluorescent image and quantified data plot for *E. coli* O157:H7, and (c) and (d) are the results for *H. pylori*. The curves show a similar trend for both antigens – signal intensity came to a peak value at a certain antigen concentration, meaning that the optimal surface density of antigen was reached. The optimal antigen concentrations were 30 μg mL^{-1} and 200 μg mL^{-1} for *E. coli* O157:H7 and *H. pylori*, respectively, under the current experimental protocol. These conditions were used for the rest of the study.

The sharp decrease of signal intensity at antigen concentrations higher than the optimum suggested reduced IA efficiency when the adsorbed antigen layer became too dense, probably due to steric inhibition and/or denature of antigen. This significant decrease of assay efficiency at elevated concentration of probing molecules has also been reported in another study of microfluidic immunoassay using native PDMS as the solid phase [21]. Therefore, it is very likely that the high avidity of PDMS for proteins [46] causes too dense a monolayer of adsorbed molecules. One disadvantage here is that the optimal surface concentration of probing molecules is reached at an unstable, transient stage during the dynamic adsorption process, rather than at equilibrium. Therefore, the coating effect can be easily affected by small variations in the experimental conditions, e.g., coating time or room temperature, thus impairing the reproducibility of the assay. One solution to this problem is to hydrophilize the PDMS, e.g., by using plasma-treatment, to lower its protein binding capacity [29,46].

Data from the three duplicates were statistically examined: variation coefficients were ~13% for stronger signals (intensity >5) and ~25% for weaker signals (intensity <5). One source of the variation was the inhomogeneity in the fluorescence signals, which suggested inhomogeneity in antigen coating, a limitation of the current antigen immobilization protocol. Other possible contributors to the variations included uncompensated non-uniform illumination, as well as slight variations in flow rates among the channels. Nevertheless, for the purposes of this proof-of-concept study, the current precision was considered adequate.

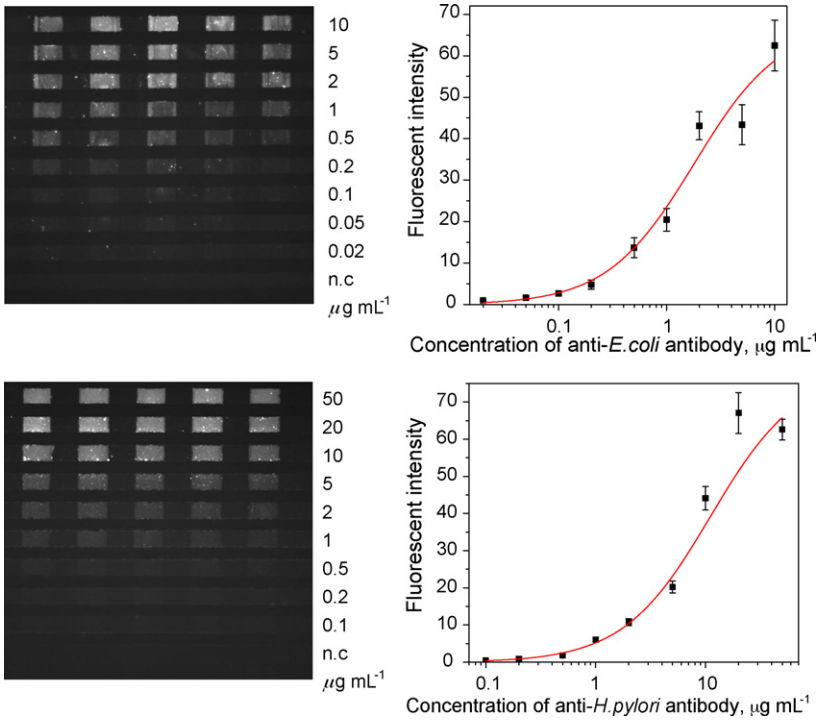

Fig. 5 – Signal intensity as a function of antibody concentration. (a) *E. coli* O157:H7 antibody concentration test. Concentrations of *E. coli* antibody were as indicated on the right hand side of the image. (b) Quantified data from (a) fitted with sigmoidal function. Error bars represent S.E.M. (c, d) Results from *H. pylori* antibody concentration test.

3.3. Dose–response curves

The microfluidic immunoassay was then evaluated by testing dynamic ranges for both analytes in synthetic samples. Five coating channels were all used for duplicate assays. The concentration ranges of sample solutions were 0.02–10 $\mu g\,mL^{-1}$ for *E. coli* O157:H7 antibody and 0.1–50 $\mu g\,mL^{-1}$ for *H. pylori* antibody. The results are shown in Fig. 5, in which (b) and (d) are quantified data fitted with sigmoidal curves. From these curves, concentration-response dependence covered the full range of tested concentrations for both analytes, with lower detection limit determined as the concentration yielding an average intensity above mean ± 3S.D. of the negative control. Shapes of the curves suggested that the dynamic ranges could be still broader, from both the lower and higher limits of testing. Nevertheless, the demonstrated dynamic range with 2–3 logs is considered wide enough, because it is typical for most ELISA in practical use [47]. The detection limits of 0.02 $\mu g\,mL^{-1}$ (130 pM) and 0.1 $\mu g\,mL^{-1}$ (670 pM) for *E. coli* O157:H7 and *H. pylori* antibodies are close to the lower limit of fluorescence immunoassays (~100 pM) [48]. These results are thus satisfactory, particularly considering that the capture antigens employed were whole cell bacterial lysates, without purification. The limits of detection achieved are also comparable to those from other microfluidic immunosensors [3].

3.4. Assay of human serum

The microfluidic assay was then applied to detect samples of human serum with known infection status of either *E. coli* O157:H7 or *H. pylori*. A major issue associated with serum testing is the adsorption of serum constituents to hydrophobic channel walls [33]. High background fluorescence was observed in our experimental trials when serum was not sufficiently diluted or when the diluent buffer was not strong enough. From an immunoassay experiment conducted with a series of dilutions of an *H. pylori*-positive serum, dilutions of 1:50, 1:100 and 1:200 yielded close signal-to-noise ratios (signal and noise being the intensity from the reaction site and the background, respectively) of ~1.38, which was better than the ratios of 1:28 and 1.19 from dilutions 1:20 and 1:500, respectively. A 1:100 serum dilution was thus used for the rest of the experiments. For the blocking/diluent buffer, 10% (w/v) BSA solution was found to suppress non-specific binding still better than 5% BSA solution and was used in the assay of serum. Other blocking agents tested, such as normal donkey serum (<10%) and Tween (0.1%, added to the BSA-contained blocking buffer), while produced even lower background signals than 10% BSA, also impaired antigen–antibody binding reactions, and, thereby, lower the signal-to-noise ratio.

Results from assay of serum are shown in Fig. 6. The five coating channels were all used to provide duplicates. A clear visual distinction existed between the fluorescent intensities from positive and negative samples, for both *E. coli* O157:H7 and *H. pylori*. Using mean ± 3S.D. of the signal intensities from negative sera as cut-off values (shown as the dotted line in Fig. 6), there was neither false-positive nor false-negative result. With one-way analysis of variance (ANOVA), statistically significant distinction ($P < 0.05$) existed between all *H. pylori*-positive and *H. pylori*-negative samples, and between the first four *E. coli*-positive samples and all *E. coli*-negative samples. Although the fifth *E. coli*-positive sample could be distinguished from only two out of the four negative samples with statistical significance, it was a weakly positive sample, with the microtitre ELISA reading closest to the cut-off value compared to the other four positive samples. The overall accuracy was thus satisfactory in using the microfluidic immunoas-

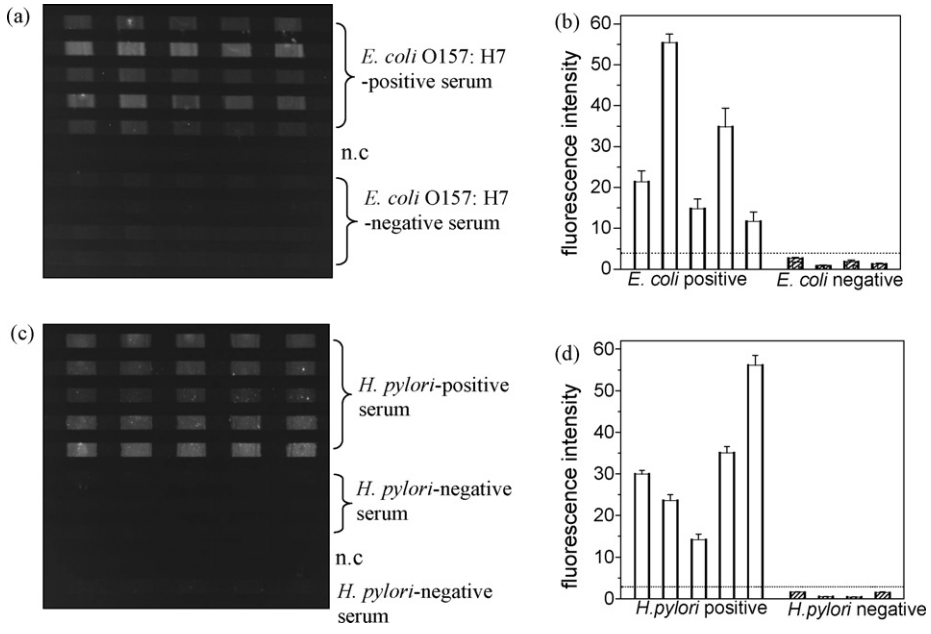

Fig. 6 – Detection of bacterial-specific antibodies from human serum. All serum samples were diluted to 1:100 using 10% (w/v) BSA-containing buffer. (a) Assay for *E. coli* O157:H7 antibody. (b) Quantified data from (a). The dotted line represents the cut-off value, calculated as mean ± 3S.D. of the signals from negative samples. (c, d) Assay for *H. pylori* antibody. The detection antibody was donkey anti-human IgG diluted using 5% (w/v) BSA for both assays.

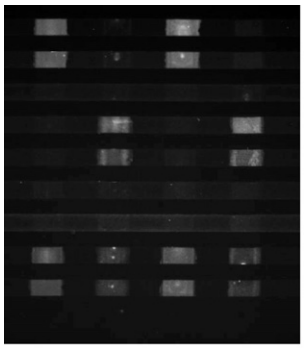

Fig. 7 – Simultaneous detection of both antibodies from human serum. Antigens of *H. pylori* and *E. coli* O157:H7 were coated alternately, as indicated at the bottom of the image. Samples are labeled from S1 to S10 and the contents of the each sample are indicated on the right side of the image. Capital "P" or "N" denotes a positive or negative sample, respectively. For S1 to S7, the dilution of serum was 1:100. S8 and S9 were mixed samples of *H. pylori*-positive and *E. coli* O157:H7-positive serum. The overall serum dilution was 1:50 for S8 and S9, in order to match the concentration of each antibody to that in the corresponding unmixed serum. For example, the concentration of *H. pylori* antibody in S1 and S8 were equivalent.

say to screen for either *E. coli* O157:H7 or *H. pylori* antibody in human serum.

The close-to-zero signal intensities of the negative sera implied that very little cross-reaction occurred between serum proteins and immobilized antigens. Also, the low background fluorescence in the images, comparable with that from assays of synthetic samples, demonstrated effective inhibition of non-specific binding of serum proteins to channel walls.

3.5. *Simultaneous screening of two target antibodies from human serum*

Simultaneous screening of both *E. coli* O157:H7 antibody and *H. pylori* antibody in synthetic samples has been briefly demonstrated in our earlier study [28]. Here, we verified the applicability of the multiplexed assay in testing human serum, with the improved high-throughput immunoassay. Fig. 7 shows the fluorescent image from the test. Duplicate antigen coatings of *H. pylori* and *E. coli* O157:H7 were applied alternately. Samples included positive and negative serum samples for each pathogen, as well as mixed samples containing both antibodies. The results demonstrate good specificity for the assay: an antigen-coating site yielded a strong fluorescent signal only when the corresponding antibody was present in the sample. This finding indicated that no cross-reactions occurred between different antibodies and antigens. Also, different samples yielded consistent fluorescent intensities for the same analyte, by comparing signals of *H. pylori* from S1 and S8, S2 and S9, or signals of *E. coli* O157:H7 from S4 and S8, S5 and S9. These results confirmed the capability of this microfluidic immunoassay for simultaneous, accurate assay of the infection status of multiple pathogens from human serum.

4. Conclusion

This study has demonstrated the proof-of-concept of a high-throughput electrokinetically-controlled heterogeneous immunoassay chip. With effective control of the microfluidic transport process in a compact microfluidic network, this microfluidic immunoassay lab-on-a-chip is capable of detecting ten samples simultaneously in 22 min. *E. coli* O157:H7 antibody and *H. pylori* antibody in buffer solutions were detected down to 0.02 $\mu g\,mL^{-1}$ (130 pM) and 0.1 $\mu g\,mL^{-1}$ (670 pM), respectively. The microfluidic immunoassay was also applied to screen for *E. coli* O157:H7 antibody or *H. pylori* antibody from human serum. In the 18 samples of human serum tested, *E. coli* O157:H7-positive or *H. pylori*-positive sera were accurately distinguished from the corresponding negative sera, mostly with statistical significance. Simultaneous screening of both antibodies from human serum was also proved feasible. With non-specific binding effectively suppressed by 10% (w/v) BSA, the assay results showed no evidence of adsorption of serum proteins to channel walls and consequent disturbance to electrokinetic transport. These results, thus, prove the applicability of electrokinetically-driven heterogeneous immunoassay chip to clinical environments.

The assay can be easily expanded in the future to test additional samples and more analytes in parallel, with the aid of numerical simulation for precise control of the microfluidic transport process in a complicated μFN. Antigen immobilization approach should also be improved for better precision and sensitivity of the assay, by using non-adsorptive methods such as covalent bonding.

Acknowledgements

This study was supported by a grant from Collaborative Health Research Project and Natural Sciences and Engineering Research Council of Canada (to D. Li and P.M. Sherman), and University of Toronto Open Fellowship (to Y. Gao). P.M. Sherman is the recipient of a Canada Research Chair in Gastrointestinal Disease. The authors thank Dr. F.Y.H. Lin for suggestions on the assay of human sera and Dr. G. Hu for help with numerical simulation.

REFERENCES

[1] P.S. Dittrich, K. Tachikawa, A. Manz, Anal. Chem. 78 (2006) 3887.
[2] P.A. Auroux, Y. Koc, A. DeMello, A. Manz, P.J.R. Day, Lab Chip – Miniaturisation Chem. Biol. 4 (2004) 534.
[3] A. Bange, H.B. Halsall, W.R. Heineman, Biosens. Bioelectron. 20 (2005) 2488.
[4] J.W. Cooper, Y. Wang, C.S. Lee, Electrophoresis 25 (2004) 3913.
[5] A.M. Dupuy, S. Lehmann, J.P. Cristol, Clin. Chem. Lab. Med.: CCLM/FESCC 43 (2005) 1291.
[6] D. Huh, W. Gu, Y. Kamotani, J.B. Grotberg, S. Takayama, Physiol. Meas., 26 (2005).
[7] N. Honda, U. Lindberg, P. Andersson, S. Hoffmann, H. Takei, Clin. Chem. 51 (2005) 1955.

[8] C.A. Rowe, S.B. Scruggs, M.J. Feldstein, J.P. Golden, F.S. Ligler, Anal. Chem. 71 (1999) 433.
[9] K.S. Kim, J.K. Park, Lab Chip – Miniaturisation Chem. Biol. 5 (2005) 657.
[10] E.P. Kartalov, J.F. Zhong, A. Scherer, S.R. Quake, C.R. Taylor, W.F. Anderson, BioTechniques 40 (2006) 85.
[11] S. Cesaro-Tadic, G. Dernick, D. Juncker, G. Buurman, H. Kropshofer, B. Michel, C. Fattinger, E. Delamarche, Lab Chip – Miniaturisation Chem. Biol. 4 (2004) 563.
[12] K. Hosokawa, M. Omata, K. Sato, M. Maeda, Lab Chip – Miniaturisation Chem. Biol. 6 (2006) 236.
[13] M. Madou, J. Zoval, G. Jia, H. Kido, J. Kim, N. Kim, in: M.L. Yarmush (Ed.), Annu. Rev. Biomed. Eng., vol. 8, 2006, p. 601.
[14] E. Yacoub-George, W. Hell, L. Meixner, F. Wenninger, K. Bock, P. Lindner, H. Wolf, T. Kloth, K.A. Feller, Biosens. Bioelectron. 22 (2007) 1368.
[15] K. Sato, M. Tokeshi, H. Kimura, T. Kitamori, Anal. Chem. 73 (2001) 1213.
[16] R.P. Sebra, K.S. Masters, C.Y. Cheung, C.N. Bowman, K.S. Anseth, Anal. Chem. 78 (2006) 3144.
[17] A.J. Haes, A. Terray, G.E. Collins, Anal. Chem. 78 (2006) 8412.
[18] K. Sato, M. Yamanaka, H. Takahashi, M. Tokeshi, H. Kimura, T. Kitamori, Electrophoresis 23 (2002) 734.
[19] S. Lai, S. Wang, J. Luo, L.J. Lee, S.T. Yang, M.J. Madou, Anal. Chem. 76 (2004) 1832.
[20] A. Bernard, B. Michel, E. Delamarche, Anal. Chem. 73 (2001) 8.
[21] M. Wolf, D. Juncker, B. Michel, P. Hunziker, E. Delamarche, Biosens. Bioelectron. 19 (2004) 1193.
[22] X. Jiang, J.M.K. Ng, A.D. Stroock, S.K.W. Dertinger, G.M. Whitesides, J. Am. Chem. Soc. 125 (2003) 5294.
[23] G.J.M. Bruin, Electrophoresis 21 (2000) 3931.
[24] A.G. Hadd, D.E. Raymond, J.W. Halliwell, S.C. Jacobson, J.M. Ramsey, Anal. Chem. 69 (1997) 3407.
[25] C.B. Cohen, E. Chin-Dixon, S. Jeong, T.T. Nikiforov, Anal. Biochem. 273 (1999) 89.
[26] N.H. Chiem, D.J. Harrison, Clin. Chem. 44 (1998) 591.
[27] A. Bromberg, R.A. Mathies, Electrophoresis 25 (2004) 1895.
[28] Y. Gao, G. Hu, F.Y. Lin, P.M. Sherman, D. Li, Biomed. Microdevices 7 (2005) 301.
[29] Y. Gao, F.Y.H. Lin, G. Hu, P.M. Sherman, D. Li, Anal. Chim. Acta 543 (2005) 109.
[30] G. Hu, Y. Gao, P.M. Sherman, D. Li, Microfluidics Nanofluidics 1 (2005) 346.
[31] Q. Xiang, G. Hu, Y. Gao, D. Li, Biosens. Bioelectron. 21 (2006) 2006.
[32] J.E. Butler, in: E.P. Diamandis, T.K. Christopoulos (Eds.), Immunoassay, Academic Press, San Diego, CA, 1996, p. 205.
[33] V. Linder, E. Verpoorte, N.F. de Rooij, H. Sigrist, W. Thormann, Electrophoresis 23 (2002) 740.
[34] P.I. Tarr, M.A. Neill, Gastroenterol. Clin. N. Am. 30 (2001) 735.
[35] P.M. Sherman, E. Hassall, R.H. Hunt, C.A. Fallone, S. Veldhuyzen Van Zanten, A.B.R. Thomson, Can. J. Gastroenterol. 13 (1999) 553.
[36] N. Uemura, S. Okamoto, S. Yamamoto, N. Matsumura, S. Yamaguchi, M. Yamakido, K. Taniyama, N. Sasaki, R.J. Schlemper, N. Engl. J. Med. 345 (2001) 784.
[37] F.Y.H. Lin, M. Sabri, D. Erickson, J. Alirezaie, D. Li, P.M. Sherman, Analyst 129 (2004) 823.
[38] F.Y.H. Lin, P.M. Sherman, D. Li, Biomed. Microdevices 6 (2004) 125.
[39] L.M. Best, S.J.O.V. Van Zanten, P.M. Sherman, G.S. Bezanson, J. Clin. Microbiol. 32 (1994) 1193.
[40] M.A. Karmali, M. Mascarenhas, M. Petric, L. Dutil, K. Rahn, K. Ludwig, G.S. Arbus, P. Michel, P.M. Sherman, J. Wilson, R. Johnson, J.B. Kaper, J. Infect. Dis. 188 (2003) 1724.
[41] C.X. Qiu, D.J. Harrison, Electrophoresis 22 (2001) 3949.
[42] E.B. Cummings, S.K. Griffiths, R.H. Nilson, P.H. Paul, Anal. Chem. 72 (2000) 2526.
[43] M. Zimmermann, E. Delamarche, M. Wolf, P. Hunziker, Biomed. Microdevices 7 (2005) 99.
[44] G. Hu, Y. Gao, D. Li, Biosens. Bioelectron. 22 (2007) 1403.
[45] A. Dodge, K. Fluri, E. Verpoorte, N.F. De Rooij, Anal. Chem. 73 (2001) 3400.
[46] J.E. Butler, E.P. Lu, P. Navarro, B. Christiansen, J. Mol. Recogn. 10 (1997) 36.
[47] D.M. Kemeny, A Practical Guide to ELISA, Pergamon Press, Elmsford, NY, 1991.
[48] R. Edwards, Immunoassay: An Introduction, William Heinemann Medical Books, London, 1985.